

Some design implications of X-ray crystal structures of SARS-CoV-2 3CL^{pro}

Martin Stoermer (email: m.stoermer@imb.uq.edu.au) and Peter W. Kenny (email: pwk.pub.2008@gmail.com)

Keywords: SARS-CoV-2, COVID-19, coronavirus, 3CL^{pro}, main protease, M^{pro}, inhibitor design.

Analysis of X-ray crystal structures

The recent release of SARS-CoV-2 3CL^{pro} [crystal structures](#) both with and without ligands bound reveals important details of the inhibitors produced to date. Two illustrative examples are shown below, both are covalent modified peptide inhibitors attached to the active site cysteine residue. In the first example PDB:[6lu7](#), a Michael acceptor warhead anchors the inhibitor irreversibly to the protein, and then makes other notable interactions in the S1, S2, and S4 subsites (Figure 1, Panel A). However, the side chain of the P3 valine produces no productive interactions, and neither does the “P5” capping isoxazole group. It should be noted that there are a range of different types of residues at P3 in the native SARS-CoV-2 [substrate sequences](#), smallish beta branched Val,Thr, hydrophobic Met, and basic Arg, Lys. It would appear likely that the Val seen in the original crystal structure is suboptimal. Whereas replacement with a polar (Tyr) or basic (Arg/Lys) residue could potentially provide additional productive interactions with the acidic S3 region. In PDB:[6y2f](#) the inhibitor is an α -ketoamide, which forms a reversible bond with the catalytic cysteine. The P3 residue has been replaced with a more rigid 3-amino-2-pyridone unit. The capping Boc group now theoretically occupies the P4 position of the inhibitor but does not occupy the S4 pocket as alanine does in PDB:[6lu7](#). Rather the Boc group is projected into solvent (Figure 1, Panel B). and makes no productive interactions with the enzyme. Instead a DMSO molecule from the crystallisation buffer occupies the S4 pocket.

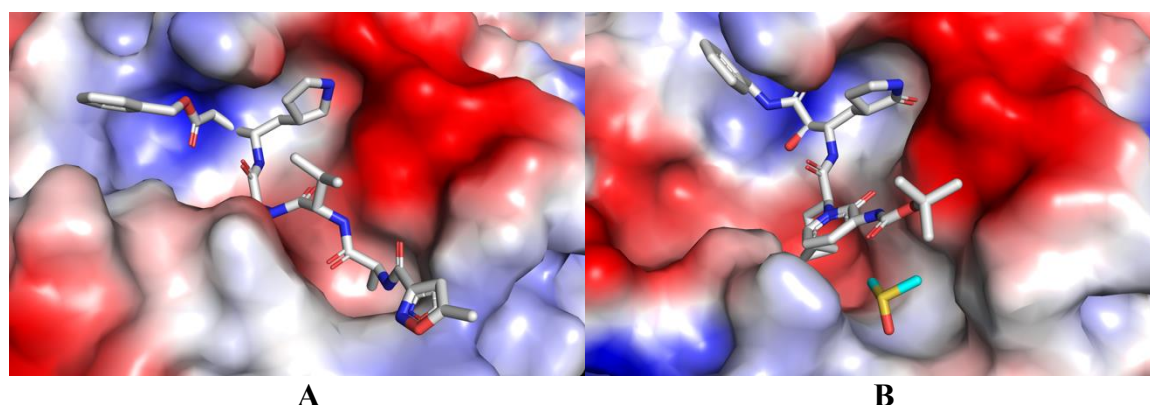


Figure 1: Electrostatic surface of SARS-CoV-2 3CL^{pro} crystal structures PDB:[6lu7](#) (Panel A) and PDB:[6y2f](#) (Panel A). Ligands shown as grey sticks, DMSO molecule shown with cyan carbons, yellow sulfur and red oxygen sticks.

Looking at more detail at the hydrogen bonding network of the P3 residue in PDB:[6lu7](#) the main chain of the P3 valine does interact as expected in a strand-strand interaction with Glu166 of the enzyme with two hydrogen bonds $\text{LigP3ValO} - \text{Glu166HN} = 2.0\text{\AA}$ and $\text{LigP3ValNH} - \text{Glu166O} = 1.9\text{\AA}$. (Figure 2, Panel A). Importantly the interacting atoms in the two hydrogen bonds are very close to being in the same plane, which is required for optimal hydrogen bonding (Panel B).

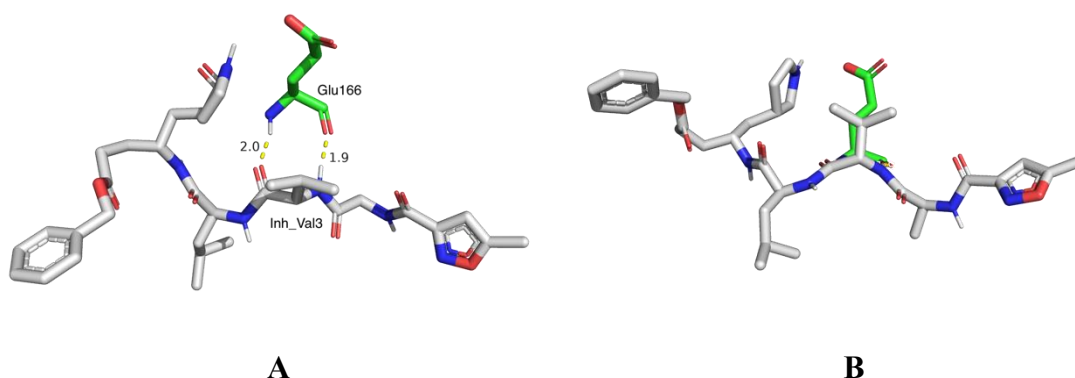


Figure 2: Top (Panel A) and side (Panel B) views of the hydrogen bonding interactions of the P3 alanine inhibitor residue with SARS-CoV-2 3CL^{pro} crystal structures PDB:6lu7. Ligand shown as grey sticks, protein residue Glu166 green sticks. The more rigid pyridone unit in the PDB:6y2f inhibitor on the other hand enforces a sub-optimal hydrogen bonding network with the protein residue Glu166 (Figure 3). Whilst the NH-O distances are good, it is the angles which deviate from the ideal.

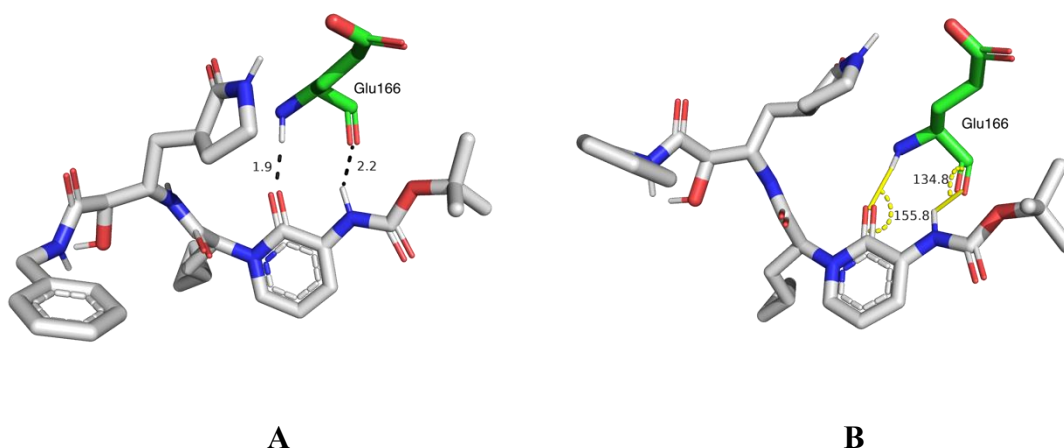


Figure 3: Hydrogen bonding interactions between the P3 aminopyridone group in the ketoamide inhibitor from PDB:6y2f. Panel A shows the short NH-O distances, Panel B illustrates the deviations from 180°

Design implications

Compound **1** inhibits the of SARS-CoV-2 3CL^{pro} with an IC₅₀ = 0.67 μM and it is stated that the inhibitory potency of compound **2** is two-fold lower. The suboptimal hydrogen bond geometry shown in Figure 3B and the potential for unfavourable [secondary electrostatic interactions](#) (e.g., between Boc-amide NH and Glu 166 amide NH) suggest that it may be possible to delete the 3-amino substituent without losing too much inhibitory potency.

Although the deletion of the 3-amino substituent of **2** removes two hydrogen bond donors from the molecular structure, it should not be automatically assumed that this will result in lower aqueous solubility. For example, a number of studies [[L2006](#) | [B2009](#) | [R2015](#)] have shown that N-methylation of secondary amides typically leads to increased aqueous solubility.

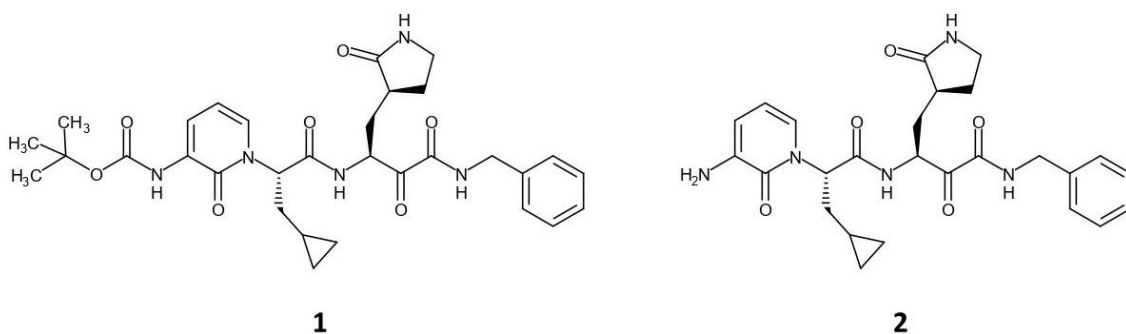


Chart 1: Structures of SARS-CoV-2 3CL^{pro} inhibitors

If deletion of the 3-amino substituent is well-tolerated then replacement of the pyridone with saturated analogs (Chart 2) can be considered and these can be further elaborated structurally if the initial structural changes are, in turn, well-tolerated. Note that a 3-amino substituent on the piperidone is likely to be protonated under assay conditions (pK_a values of 7.9 and 7.8 respectively have been [reported](#) for glycine amide and glycine methyl ester).

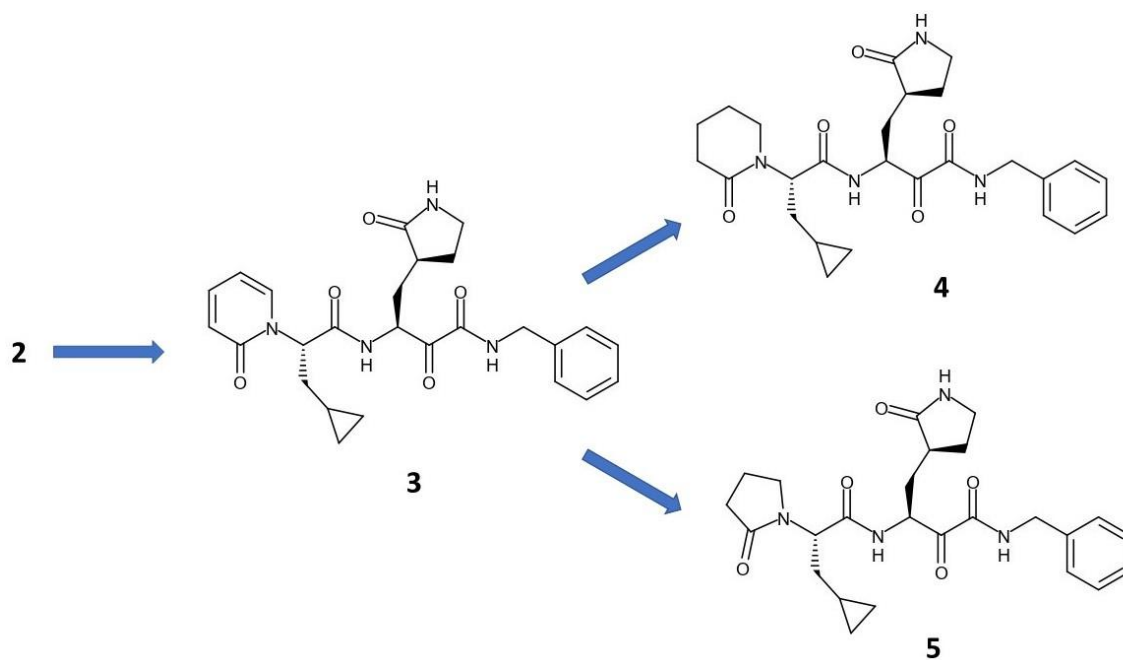


Chart 2: Deletion of 3-amino substituent of **2** as a design tactic